Reconstruction of bio-conductivity distribution from tangential magnetic field measurements

C. Sumi and K. Nagumo

Department of Electrical and Electronics Engineering, School of Science and Technology,

Sophia University, Tokyo 102-8554, JAPAN

Abstract **We proposed a technique for reconstructing bio-electric conductivity distribution from measured tangential magnet field data. That is, in the 2D ROI with an arbitrary depth two orthogonal tangential components of 3D current vector field were respectively estimated from the synthetically measured two tangential magnetic fields, from which the 2D conductivity distribution was estimated. To cope with inevitable measurement errors, a robust numerical solution was developed, in which the mollification method and the regularization method were efficiently utilized. By performing this 2D reconstruction at each depth, 3D conductivity distribution could be estimated. As typical applications, pathological state and/or bio-electric conductive path can be evaluated by monitoring the temporal change of the reconstructed 3D conductivity distribution. The feasibility of this technique was briefly verified by reconstructing a conductivity distribution using simulated noise-filled magnetic field data, with resultant reconstructions indicating that the approach could provide a practical means for robustly reconstructing a conductivity distribution.**

Keywords: 3D conductivity distribution, inverse problem, tangential magnetic vector fields, fewer measurements, first-order partial differential equations, finite-difference method, mollification method, regularization method, tangential current vector fields, lead field

I. Introduction

Utilizing SQUID magnetometer, ferromagnetic particles or electrical activities are evaluated (e.g., dust in lung [1], magnetocardiogram (MCG) [1, 2], magnetomyogram (MMG) [3], and magnetenchepharogram (MEG) [1]: visually evoked [4], auditory evoked [5], somatosensory evoked [6], spontaneous motion-related [7], cognition-related [8], and electromagnetically excited neuron- and nerve-induced [9]). Often, by modeling tissue as a conductor, current sources [10, 11, 12, 13] or current fields [2, 9, 14, 15, 16-18] are estimated. Various current field estimation techniques are developed (e.g., the unique minimum-norm least-squares estimation method [14, 18], the Wiener estimation method [15], the Fourier's filtering-based method [16, 17]). From the measured normal magnetic field to the reconstruction plane, any current field components cannot be determined [2, 9, 14, 16]. Then, the tangential magneticometer [3, 19, 20, 21] is utilized [17, 18]. That is, utilization of the magnetic fields of orthogonal two tangential components realizes unique determination of the 2D current vector field.

Recently, on 3D object the synthetic aperture technique is applied to the normal magnetic field measurement [22]. Thus, novel application of the synthetic aperture technique to the tangential magnetic field measurements could allow determination of the 3D fields of orthogonal two tangential components of 3D current vector field. In this report, to allow providing the quantitative information about the pathological state and/or bio-electric conductive path (e.g., neural networks etc), we present a reconstruction technique for monitoring the temporal change of the 3D conductivity distribution using only the estimated tangential current field data. We previously proposed a differential type conductivity inverse problem using either current or potential field data [23-25], in which, if no current sources exist in the region of interest (ROI), with respect to reference conductivity values provided in an arbitrary point [23, 24] or regions [25] the spatial distribution globally of the relative values can be determined from measured sufficient number of independent fields of another physical variable in that region. Thus, compared with an eddy current model [26] previously proposed in the field of NDE, in principle our technique can deal with an arbitrary geometry of the target and arbitrary current sources existing outside ROI. Furthermore, we delineated that proper configurations of *the reference regions and the externally situated current sources* allow reducing the required number of independent current field measurements for uniquely determining the conductivity distribution [25]. This approach is particularly effective in this case when an inherent current flow exists there and a fewer field measurements are required. In real-world applications, however, the problem inevitably becomes ill-posed due to inevitable measurement errors [24] and improper configurations [45] making it impossible to guarantee the existence of a stable and unique target global distribution. However, the demonstrated ability using simulated noise-filled current field data under the improper configurations of our developed numerical-based

Report Documentation Page

Report Date	Report Type	Dates Covered (from... to)
25OCT2001	N/A	-

Title and Subtitle Reconstruction of bio-conductivity distribution from tangential magnetic field measurements	**Contract Number**
	Grant Number
	Program Element Number
Author(s)	**Project Number**
	Task Number
	Work Unit Number
Performing Organization Name(s) and Address(es) Department of Radiology Duke University Medical Center, NC	**Performing Organization Report Number**
Sponsoring/Monitoring Agency Name(s) and Address(es) US Army Research, Development & Standardization Group (UK) PSC 802 Box 15 FPO AE 09499-1500	**Sponsor/Monitor's Acronym(s)**
	Sponsor/Monitor's Report Number(s)

Distribution/Availability Statement
Approved for public release, distribution unlimited

Supplementary Notes
Papers from the 23rd Annual International Conference of the IEEE Engineering in Medicine and Biology Society, 25-28 OCT 2001, Istanbul, Turkey. See also ADM001351 for entire conference on cd-rom.

Abstract

Subject Terms

Report Classification unclassified	**Classification of this page** unclassified
Classification of Abstract unclassified	**Limitation of Abstract** UU

Number of Pages
6

implicit-integration approach to reconstruct the globally relative conductivity distribution is concluded to confirm the potential value that it can yield the acceptable unique reconstruction even when fewer field measurements are unfortunately taken [44]. To cope with inevitable measurement errors, in conjunction with the synthetic aperture technique a robust current field estimation method was developed, in which the mollification method and the regularization method were efficiently utilized. By enhancing and combining the current estimation method and the conductivity estimation method, we obtained the 3-D conductivity reconstruction technique. The feasibility of the technique is evaluated by reconstructing a globally relative conductivity distribution using simulated noise-filled magnetic data, with resultant reconstructions indicating that the approach provides a practical means for robustly reconstructing conductivity distribution.

II. Conductivity reconstruction technique

The conductive target medium existing in 3D space expressed by Cartesian coordinate system (x, y, z) has 3D conductivity distribution $\sigma(x, y, z)$. The 3D ROI Ω is taken into the target medium. The conductivity distribution $\sigma(x, y, z)$ in Ω is spatially smooth, and the reference conductivity values σ_l ($l = 1, \ldots, N$) are provided in reference regions ω_l existing in Ω, i.e.,

$$\ln \sigma(x, y, z) = \ln \sigma_l, \quad (x, y, z) \in \omega_l \quad (l = 1, \ldots, N). \qquad (1)$$

Under the conditions, magnetic field $\mathbf{B}(x, y, z)$ (= (Bx (x, y, z), By(x, y, z), Bz (x, y, z))^T) is generated by 3D current density field $\mathbf{J}(x,y,z)$ (= (Jx (x, y, z), Jy (x,y,z), Jz (x, y, z))^T) due to arbitrary current sources existing inside and/or outside the ROI Ω. Here, we assume that the following first-order PDEs hold in Ω for the 3D quasi-relative conductivity distribution $\ln\sigma(x, y, z)$ [23], i.e.,

$$\nabla \times \mathbf{J}(\mathrm{x}, \mathrm{y}, \mathrm{z}) + \nabla \ln(1/\sigma(x, y, z)) \times \mathbf{J}(\mathrm{x}, \mathrm{y}, \mathrm{z}) = \mathbf{0}. \qquad (2)$$

If synthetic measurements could be taken at the infinite plane of $\{z = z_0, -\infty \le x \le \infty, -\infty \le y \le \infty\}$ over the medium without no errors on the magnetic field components Bx (x, y, z_0; Z) and By (x, y, z_0; Z) respectively generated by the current density field components Jy (x, y, Z) and Jx (x, y, Z) in an arbitrary plane of $z = Z$ in the target medium, by mathematically resolving the Biot-Savart's law [16, 17], i.e.,

$$\mathrm{B}(x,y,z_0;Z) = \int_{z'=Z, -\infty \le x' \le \infty, -\infty \le y' \le \infty} \frac{\mu}{4\pi} \mathbf{J}(x', y', z') \times \frac{\mathbf{r}}{|\mathbf{r}|^3} dS, \qquad (3)$$

the 2D fields of the components Jx (x, y, Z) and Jy (x, y, Z) of the 3D flow can be uniquely determined, where permeability μ is the given spatial function, and $\mathbf{r}$ is the distance vector from (x', y', Z) to (x, y, z_0). That is, in this ideal case, by performing the Fourier's analysis on every plane the 3D fields of the components Jx (x, y, z) and Jy (x, y, z) can be uniquely determined. Thus, in practice, coordinate system should be taken such that generated current flow is dominant in the estimation plane.

To determine the 3D conductivity distribution $\sigma(x, y, z)$, one of three PDEs (2) is handled for every plane, i.e., for the plane of $z = Z$,

$$\left(\mathrm{Jy}(x,y,Z) \quad -\mathrm{Jx}(x,y,\mathrm{Z})\right) \begin{pmatrix} \frac{\partial}{\partial x} \ln\sigma(x,y,Z) \\ \frac{\partial}{\partial y} \ln\sigma(x,y,Z) \end{pmatrix} = \frac{\partial}{\partial x}\mathrm{Jy}(x,y,Z) + \frac{\partial}{\partial \mathrm{y}}\mathrm{Jx}(x,y,Z). \qquad (4)$$

When in the plane only single current field of components Jx (x, y, Z) and Jy (x, y, Z) can be measured, to allow unique determination of the 2D conductivity distribution $\ln\sigma(x, y, Z)$, the reference regions crossing ω_l (l = 1, … , N) must extend in the parallel direction of the imitated 2D current flow (Jx (x, y, Z), Jy (x, y, Z))^T [25]. Fortunately, if measurements of two independent current fields $\mathbf{J}_1(x, y, z)$ and $\mathbf{J}_2(x, y, z)$ can be taken, correspondingly derived two PDEs are handled as simultaneous equations [23, 24]. In this case, existence in the plane of only a reference point enables the unique determination [23].

In practice, however, to determine the current field components Jx (x, y, Z) and Jy (x, y, Z) in the finite 2D ROI Ω_Z, i.e., the finite 2D region of $z = Z$ in the 3D ROI Ω, measurements of the magnetic field components Bx (x, y, z_0; Z) and By (x, y, z_0; Z) are performed in the finite 2D region of $z = z_0$ over the discrete 2D ROI Ω_K on a discrete Cartesian coordinate system (i, j, K) in which i, j, and K are arbitrary integers respectively satisfying (x, y, Z) $\cong$ ($i\Delta x$, $j\Delta$y, $K\Delta z$) with respect to the sufficiently small spatial increments Δx, Δy, and Δz in the x-, y-, and z-directions. As the measured magnetic field data Bx (i, j, k_0; K) and By (i, j, k_0; K) ($k_0 = z_0 / \Delta z$) are contaminated with measurement errors, the current field components Jx (i, j, K) and Jy (i, j, K) are estimated in the numerical least squares sense. Here, one should note that the current sources/current flow outside the ROI Ω significantly contributes to magnetic fields over the neighborhood of the border of Ω; then resulting in the estimation errors in $\mathbf{J}$ (i, j, K). Thus, the extra contributions in Bx (i, j, k_0; K) and By (i, j, k_0; K) are reduced by being windowed with the weight function W(i, j, k_0;

K), i.e., the spatial function having absolute values of the magnetic field **B** (*i, j, k*$_0$; *K*) calculated from uniform 2D current flow with unity magnitude in an arbitrary direction in the 2D ROI Ω_K. In addition to the fact that the current field components Jx (*i, j, K*) and Jy (*i, j, K*) and their 2D gradients are bounded, utilization of the regularization method under the assumption of the boundness of their 2D Laplacians enables stable estimation of the 3D fields of Jx (*i, j, k*) and Jy (*i, j, k*). That is, minimization is performed in every 2D ROI Ω_K of the following functional with respect to the raw vector **J** comprised of both the unknown current densities Jx (*i, j, K*) and Jy (*i, j, K*), i.e.,

$$R_J(\mathbf{J}) = \|\mathbf{B_W} - \mathbf{LJ}\|^2 + \alpha_{J1}\|\mathbf{J}\|^2 + \alpha_{J2}\|\mathbf{DJ}\|^2 + \alpha_{J3}\|\mathbf{D}^T\mathbf{DJ}\|^2, \quad (5)$$

where the raw vector $\mathbf{B_W}$ is comprised of the lexicographically ordered windowed magnetic data W(*i, j, k*$_0$) Bx (*i, j, k*$_0$; *K*) and W(*i, j, k*$_0$) By (*i, j, k*$_0$; *K*), the matrix **L** is of the lead field data, the matrix **D** is of coefficients of employed first-order approximations of 2D partial derivatives of Jx (*i, j, K*) and Jy (*i, j, K*), and α_{J1}, α_{J2}, and α_{J3} are so-called regularization parameters adjusting the relative weights for $R_J(\mathbf{J})$ of the correspondingly derived penalty terms, i.e., L_2 norms of **J**, of the 2D gradient, and of the 2D Laplacian. Providing that α_{J1}, α_{J2}, and α_{J3} are large enough, due to (5) being positive-definite, the minimization is stably performed. Thus, with high SNRs reasonably smoothed 2D current field data Jx (*i, j, K*) and Jy (*i, j, K*) are obtained.

Utilization of the obtained smooth current field data Jx (*i, j, K*) and Jy (*i, j, K*) and their 2D spatial derivatives calculated by applying the differential filter [23] with an appropriate cut-off frequency fc to the current filed data, high SNR approximations of the spatially inhomogeneous coefficients in (4) are obtained. Furthermore, by approximating the 2D gradient operator using the first-order finite difference, over each 2D ROI Ω_K the first-order finite-difference equations with the approximations of the inhomogeneous coefficients are derived with exception of the some boundary points of Ω_K [24, 25]. Subsequently, by substituting the reference values $\ln\sigma_l$ into the finite-difference equations representing $\ln\sigma$ (*i, j, K*) in Ω_K crossing ω_l (*l* = 1,…, *N*), the following system of equations are derived to determine the unknown 2D global solution **s**, i,e., a raw vector comprised of unknown globally relative conductivities $\ln\sigma$ (*i, j, K*) in Ω_K:

$$\mathbf{J\,D'\,s} = \mathbf{j}, \quad (5)$$

where the matrix **J** is comprised of the reasonably smoothed current densities, the matrix **D'** of coefficients of the first-order approximations of 2D partial derivatives of $\ln\sigma$ (*i, j, K*), and the raw vector **j** of reasonably smoothed partial derivatives of the current densities. Here, we should keep in mind that, **D's** is designed to express the 2D locally relative conductivity distribution [24].

However, the current field data and their spatial derivatives in **J** and **j** has remaining estimation errors. Moreover, when only a single current field measurement is taken, configurations of current sources and reference regions might be improper ones [25]. That is, in some 2D ROIs reference regions crossing ω_l (*l* = 1, … , *N*) may be short in the parallel direction to the imitated 2D current flow. Such configurations lead to inaccessible regions in 2D ROIs; thus resulting in **JD'** being numerically singular. These current estimation errors and improper configurations are coped with by utilizing the *a priori* knowledge about the smoothness of the target distribution $\ln\sigma$ (*x, y, z*).

As the employed gradient operator **D'** has a unique least-squares inverse $(\mathbf{D'^TD'})^{-1}\mathbf{D'^T}$ with respect to the locally relative 2D conductivity distribution **D's**, by utilizing the regularization method, we just only make the distribution **D's** unique and smooth enough to be integrable over the 2D ROI Ω_K. That is, in addition to utilizing the fact that the original 2D distribution $\nabla \ln\sigma$ (x,y,Z) is bounded, since it is assumed that $\nabla \ln\sigma$ (x,y,Z) is spatially smooth, we obtain the following functional with respect to the 2D global distribution **s**:

$$R_s(\mathbf{s}) = \|\mathbf{j} - \mathbf{JD's}\|^2 + \alpha_{s1}\|\mathbf{D's}\|^2 + \alpha_{s2}\|\mathbf{D'^T\,D's}\|^2, \quad (6)$$

where α_{s1} and α_{s2} are the regularization parameters of the penalty terms, i.e., L_2-norms of the gradient and Laplacian of **s**. Due to the functional (6) derived in each 2D ROI Ω_K being positive-definite even though some 2D ROIs have originally inaccessible regions, numerical minimization of the every functional yields the 3D globally relative conductivity distribution through stable implicit-integration over an arbitrary path of the 2D locally relative conductivities [23, 24].

Minimization of functionals $R_J(\mathbf{J})$ [(5)] and $R_s(\mathbf{s})$ [(6)] are performed by the conjugate gradient method [23, 24]. Occasionally the respective minimization will be performed in 3D ROI Ω by utilizing the approximation of 3D gradient operator. The suitability of this combined current estimation method and conductivity estimation method are evaluated in the next section.

III. Evaluations

Measured tangential magnetic field data Bx (*i, j, k*$_0$) and By (*i, j, k*$_0$) are simulated by current flow in the (*x, y*)-plane with *z* = *Z* containing a central circular region (dia. = 10.0) whose conductivity value differs from that of the surrounding medium, i.e., 4.00 versus 1.00. Specifically, the current flow is generated by applying current with the intensity of 1.00 in the *x*-direction at infinite distance, and the resultant fields Bx (*x, y, z*$_0$) and By (*x, y, z*$_0$) are supposedly measured at the distance from 0.2 to 1.0 over a finite ROI {Ω_K: $-20 \le i \le 20, -20 \le j \le 20$} using $\Delta x = \Delta y = 1.0$. The magnetic fields Bx (*i, j, k*$_0$) and By (*i, j, k*$_0$) are filled with

independent white noises of the same power, and are used to estimate the current density fields Jx (*i, j, K*) and Jy (*i, j, K*). The SNRs of the simulated magnetic field data By (*i, j,* K) are 50, 40, 30, 20, and 10 dB. Subsequently, the globally relative conductivity distribution ln σ (*i, j, K*) in Ω_K taken to have a proper configuration of a reference region with respect to the applied current, i.e., {-20 $\leq$ *i* $\leq$ 20, *j* = -20}.

In the respective regularization processes in (5) and (6), we only use the preferable *a priori* knowledge about **J** and **D's**. That is, α_{J1} and α_{J2} in (5), and α_{s1} in (6) are always set equal to zeros though α_{J3} and α_{s2} are varied. In the conjugate gradient method, the initial estimates of **J** and **s** are set as a spatial distributions of zeros.

To evaluate the accuracy of estimated **J** (*i, j, K*) and ln σ (*i, j, K*), we use SNRs defined as

$$\mathrm{SNR}[P(i,j,K)] = 10\log_{10}\frac{\sum_{(i,j)\in\Omega_k}|\hat{P}(i,j,K)|^2}{\sum_{(i,j)\in\Omega_K}|\hat{P}(i,j,K)-P(i,j,K)|^2}, \quad (7)$$

where $\hat{P}$ (*i, j, K*) and P (*i, j, K*) represent the calculated and original distributions, respectively.

Effectiveness of windowing on current field estimation is shown in Fig. 1, i.e., SNRs with no application of the regularization method of the estimated current fields Jx (*i, j*) and Jy (*i, j*) vs. the distance of the sensor array from the 2D ROI, where the SNR of the no windowed magnetic field data By (*i, j*) is a parameter: ∞ dB (raw data), 40 dB, and 10dB. Obviously, windowing is effective particularly when the SNRs of magnetic data is high. The distance increasing, the accuracy of the estimation significantly degrades. Figures. 2a and 2b respectively show Bx (*i, j*) (40dB) and By (*i, j*) (16.1 dB) when the distance being 1.00, while Fig. 2c shows windowed By (*i, j*). Figures. 2d and 2e are respectively current fields Jx (*i, j*) (20.0 dB) and Jy (*i, j*) (- 0.597 dB) estimated from the windowed magnetic field data, while Fig. 2f shows Jx (*i, j*) estimated from no windowed magnetic data.

Effectiveness of regularization on current field estimation is shown in Fig. 3, i.e., regularization parameter values vs. SNRs of the estimated current fields. The estimates Jx (*i, j*) and Jy (*i, j*) obtained with the best regularization parameter value and with no regularization are shown in Figs. 2e-h, 6c-f, 7c-f, and 8c-f respectively when the SNRs of By (*i, j*) are 40, 30, 20, and 10 dB.

Effectiveness of regularization on conductivity estimation is shown in Figs. 4 and 5, i.e., regularization parameter values vs. SNRs of the estimated conductivity distributions, and SNR of By (*i, j*) vs. mean values of the best estimated conductivity values at the central squared region (3 x 3) of the inhomogeneous circular region. The best reconstructions σ (*i, j*) and the reconstructions with no regularization are shown in Figs. 2ij, 6gh, 7gh, and 8gh respectively when the SNRs of By (*i, j*) are 40, 30, 20, and 10 dB.

IV. Conclusions

In this simulation, to quantitatively evaluate the inhomogeneous conductivity value, synthetic aperture technique should realize the accurate measurements of tangential magnetic fields with SNRs larger than 30 dB [(7)] though the inhomogeneous circular region could be detected even when the SNRs of the magnetic field data are very low.

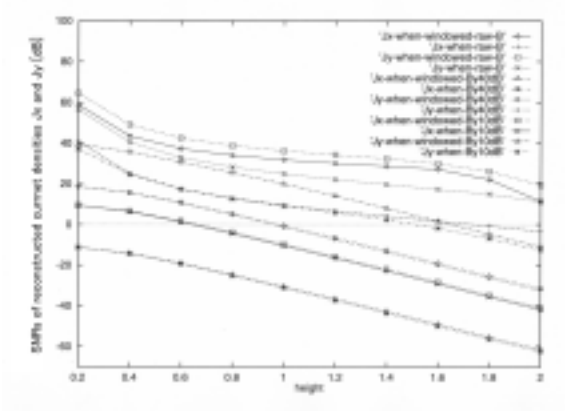

Figure. 1: SNRs of the estimated current densities vs. positioned height of magnetic sensor array.

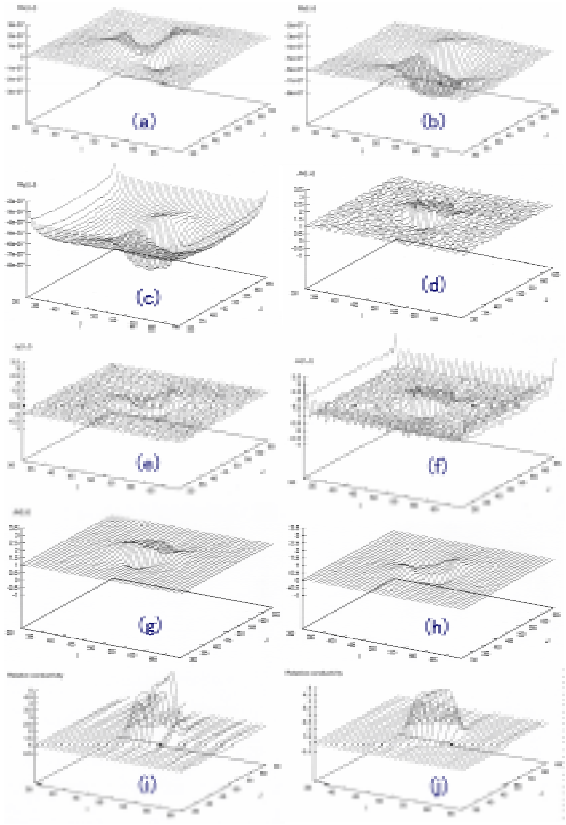

Figure. 2: Current/conductivity estimation when the distance being 1.0 and the SNR of By (*i*, *j*) being 40 dB: (a) Bx (*i*, *j*), (b) By (*i*, *j*), (c) windowed By (*i*, *j*), (d) Jx (*i*, *j*) and (e) Jy (*i*, *j*) obtained from windowed magnetic field data with no regularization, (f) Jx (*i*, *j*) obtained from no windowed magnetic data, (g) Jx (*i*, *j*) and (h) Jy (*i*, *j*) obtained with regularization from windowed magnetic data, (i) σ (*i*, *j*) obtained with no regularization from the current field data (g) and (h), (j) σ (*i*, *j*) obtained with regularization.

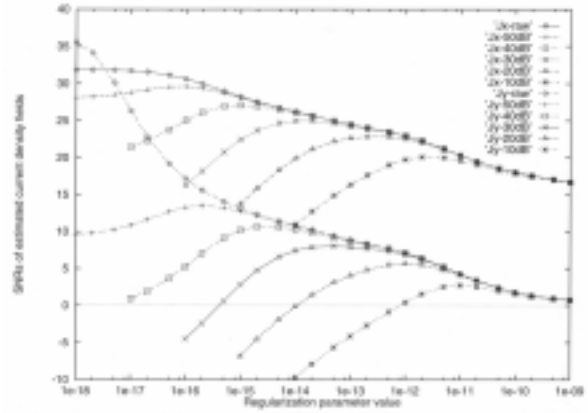

Figure. 3: Regularization parameter values vs. SNRs of the estimated current density fields.

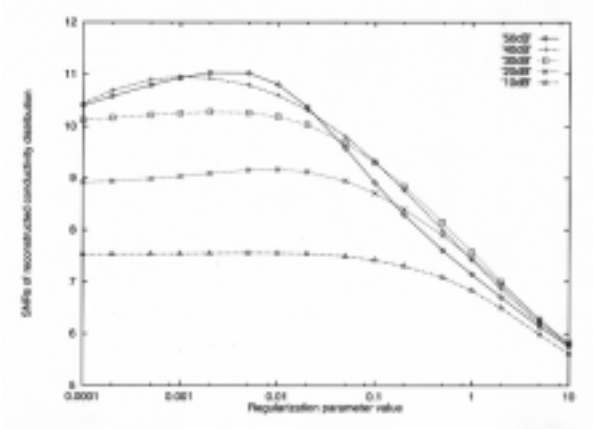

Figure. 4: Regularization parameter values vs. SNRs of the estimated conductivity distributions.

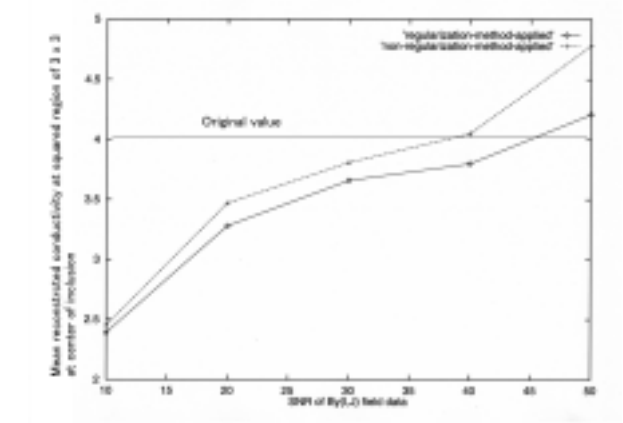

Figure. 5: SNR of By (*i*, *j*) vs. mean value of the best estimated conductivity values at central squared region (3 x 3) of the inhomogeneous circular region.

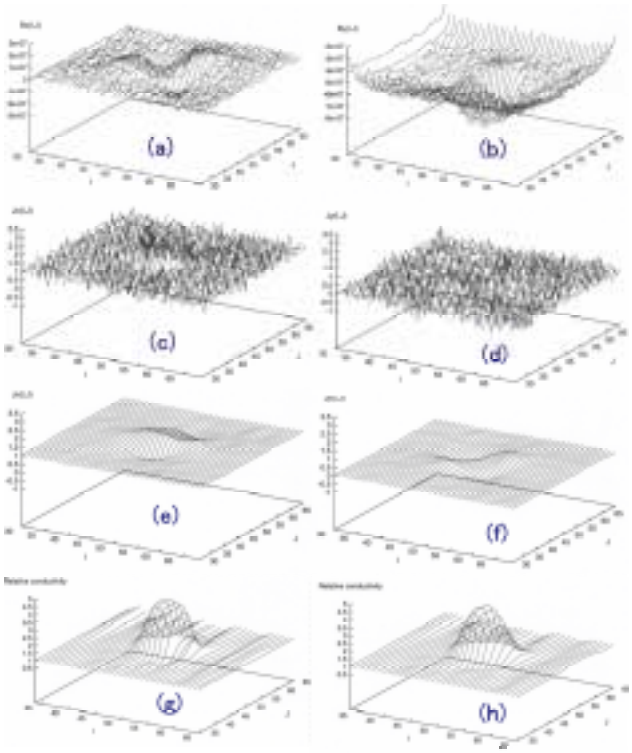

Figure. 6: Current/conductivity estimation from windowed magnetic field data when the SNR of By (*i*, *j*) being 30 dB (distance: 1.0): windowed (a) Bx (*i*, *j*) and (b) By (*i*, *j*), (c) Jx (*i*, *j*) and (d) Jy (*i*, *j*) obtained with no regularization, (e) Jx (*i*, *j*) and (f) Jy (*i*, *j*) obtained with regularization, (g) σ (*i*, *j*) obtained with no regularization from current field data (e) and (f), (h) σ (*i*, *j*) obtained with regularization.

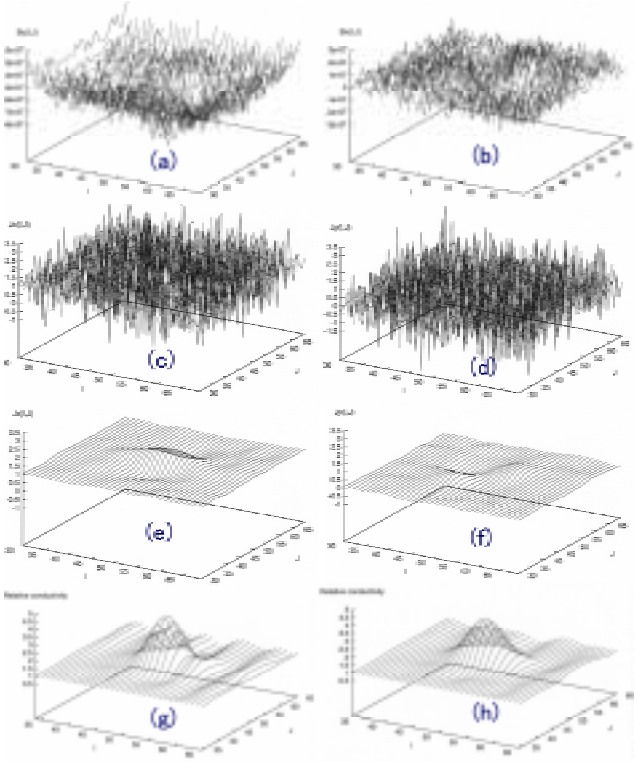

Figure. 7: Current/conductivity estimation, the SNR of By (*i*, *j*) being 20 dB.

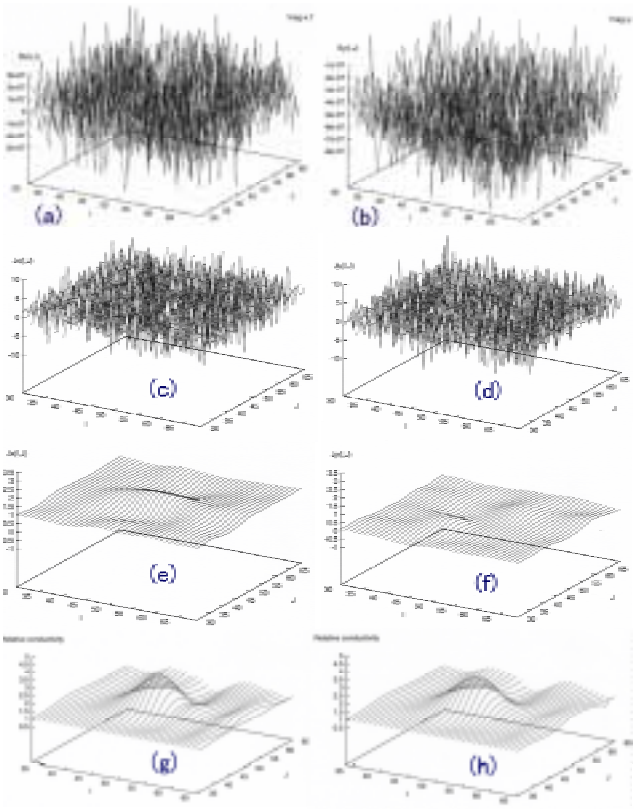

Figure. 8: Current/conductivity estimation, the SNR of By (i, j) being 10 dB.

References

[1] D. Cohen, "Measurement of the mamgnetic fields produced by the human heart, brain, and lungs," IEEE Trans. on Magn., vol. 11, no. 2, pp. 694-700, 1975.

[2] H. Hosaka, D. Cohen, B. N. Cuffin, B. M. Horacek, "The effect of the torso boundaries on the magnetocardiogram," J. Electrocardiology, vol. 9, no. 4, pp. 418-425, 1976.

[3] J. P. Wikswo, Jr., J. V. Egeraat, Y. P. Ma, N. G. Sepulveda, D. J. Staton, S. Tan, and R. S. Wijesinghe, "Instrumentation and techniques for high-resolution magnetic imaging," Proceedings of SPIE, vol. 1351, pp. 438-470, 1990.

[4] D. Brenner, J. S. Williamson, and L. Kaufman, "Visually evoked magnetic fields of the human brain," Science, vol. 190, pp. 480-482, 1975.

[5] C. Elberling, C Bak, et al., "Magnetic auditory responses from the human brain," Scand. Audiol., vol. 9, pp. 185-190, 1980.

[6] D. Brenner, J. Lipton, and L. Kaufman, and S. J. Williamson, "Somatically evoked magnetic fields of the human brain," Science, vol. 199, pp. 81-83, 1978.

[7] K. Sasaki, H. Gemba, A. Nambu, K. Jinnai, et al., "Cortical activity specific to no-go reaction in go/no-go reaction time hand movement with color discrimination in monkeys and human subjects," Biomed. Res., vol. 13 (Suppl. 1), pp. 5-9, 1992.

[8] R. Salmelin, R. Hari, O. V. Lounasmaa, M. Sams, "Picture naming --- Dynamics of brain activation," Nature, vol. 368, no. 6470, pp. 463-465, Mar. 1994.

[9] S. Kuriki, Y. Mizutani, Y. Isobe, "Transient and continuous responses of neuromagnetic fields evoked by peripheral nerve stimulation," IEEE Trans. on Magn., vol. 23, pp. 1068-1071, 1987.

[10] J. Sarvas, "Basic mathematical and electromagnetic concepts of the biomagnetic inverse problem," Phys. in Med. and Biol., vol. 32, no. 1, pp. 11-22, 1987.

[11] B. N. Cuffin, "A comparison of moving dipole inverse solutions using EEG's and MEG's," IEEE Trans. on Biomed. Eng., vol. BME-32, pp. 905-910, 1985.

[12] J. T. Nenonen, M. S. Hamlaainen, and R. J. Ilmoniemi, "Minimum-norm estimation in a boundary-element torso model," Med. and Biol. Eng. and Comput., vol. 32, pp. 43-48, 1994.

[13] K. Sekihara, D. Poeppel, A. Marantz, H. Koizumi, and Y. Miyashita, "MEG spatio-temporal analysis using a covariance matrix calculated from nonaveraged multiple-epoch data," IEEE Trans on Biomed. Eng., vol. 46, no. 5, pp. 515-521, 1999.

[14] J.-Z. Wang, S. J. Williamson, and L. Kaufman, "Magnetic source images determined by a lead-field analysis: The unique minimum-norm least-squares estimation," IEEE Trans. on Biomed. Eng., vol. 39, pp. 665-675, 1992.

[15] B. Jeffs, R. Leahy, and M. Singh, "An evaluation of methods for neuromagnetic image reconstruction," IEEE Trans. Biomed. Eng., vol. 34, pp. 713-723, 1987.

[16] B. Roth, N. G. Sepulveda, and J. P. Wikswo, Jr., "Using a magnetometer to image a two-dimensional current distribution," J. Appl. Phys., vol. 65, no. 1, pp. 361-372, 1989.

[17] A. Kandori, K. Tsukada, Y. Haruta, Y. Noda, Y. Terada, T. Mitsui, and K. Sekihara, "Reconstruction of two-dimensional current distribution from tangential MCG measurement," Phys. in Med. and Biol., vol. 41, pp. 1705-1716, 1996.

[18] C. Ramon, et al., "Simulation studies of biomagnetic computed tomography," IEEE Trans. on BME, vol. 40, no. 4, pp. 317-322, 1993.

[19] R. Grimberg, A. Savin, E. Radu, and O. Mihalache, "Nondestructive evaluation of the severity of discontinuities in flat conductive materials by an eddy-current transducer with orthogonal coils," IEEE Trans. on Magn., vol. 36, no. 1, pp. 299-307, 2000.

[20] A. Rosen, and G T Inouye, "A study of the vector magnetocardiographic waveform," IEEE Trans. on Biomed. Eng., vol. 22, pp. 167-174, 1975.

[21] K. Tsukada, Y. Haruta, A. Adachi, H. Ogata, T. Komuro, T. Ito, Y. Takada, and A. Kandori, "Multichannel SQUID system detecting tangential components of the cardiac magnetic field," Rev. Sci. Instrum., vol. 66, no. 10, pp. 5085-5091, 1995.

[22] A. A. Fife, J. Vrba, S. E. Robinson, G. Anderson, K. Betts, M. B. Burbank, D. Cheyne, T. Cheung, S. Govorkov, G. Haid, V. Haid, C. Hunter, P. R. Kubik, S. Lee, J. McKay, E. Reichl, C. Schroyen, I. Sekachev, P. Spear, B. Taylor, M. Tillotson, and W. Sutherling, "Synthetic gradiometer systems for MEG," IEEE Trans. on Appl. Supercond., vol. 9, no. 2, pp. 4063-4068, 1999.

[23] C. Sumi, A. Suzuki, and K. Nakayama, "Determination of the spatial distribution of a physical parameter from the distribution of another physical variable --- A differential inverse problem," J. Appl. Phys., vol. 70-II, no. 7, pp. 1-7, 1997.

[24] C. Sumi, and N. Tohya, "Robust reconstruction of a globally relative physical parameter distribution using measurements of another physical variable: resolution of the conductivity determination problem," Meas. Sci. and Technol., vol. 11, 795-800, 2000.

[25] C. Sumi, and H. Kou, "Robust reconstruction of a physical parameter distribution using fewer field measurements of another physical variable: resolution of conductivity determination problem," Meas. Sci. and Technol., vol. 12, no. 5, pp. 589-596, 2001.

[26] H. A. Sabbagh and L. D. Sabbagh, "An eddy-current model for three-dimensional inversion," IEEE Trans. on Magn., vol. 22, pp. 282-291, 1986.